

theropod dinosaurs.

The absence of respiratory turbinates in theropod dinosaurs indicates that they were likely to have maintained ectotherm-like resting, or routine, lung ventilation and metabolic rates (14). As in extant reptiles (for example, *Varanus*), costal breathing seems adequate to have supported active rates of oxygen consumption in such animals. Consequently, on the basis of the physiology of extant, fully terrestrial ectotherms, the necessity for a specialized diaphragm to supplement costal lung ventilation in theropods would seem anomalous. However, recent analysis suggests that expansion of lung ventilatory capacity might have allowed the relatively unmodified septate lungs of dinosaurs to have achieved active rates of O₂-CO₂ exchange that might have approached, or even overlapped, those of a few extant mammals (15). Perhaps the presence of diaphragm-assisted lung ventilation in theropods indicates that, although these dinosaurs maintained ectotherm-like routine metabolic rates, they were, nevertheless, capable of sustaining active oxygen consumption rates and activity levels well beyond those of even the most active living reptiles. Such a pattern of metabolic physiology is unknown in extant tetrapods.

This pattern of metabolic physiology in theropods might seem inconsistent with the presence of a hepatic-piston diaphragm in extant crocodylians, none of which appears to have particularly enhanced capacity for oxygen consumption during exercise (16). However, relatively low aerobic capacity in recent crocodylians, all of which are aquatic, might not represent the ancestral condition. Early (Triassic) crocodylomorphs (for example, *Protosuchus* and *Terrestriusuchus*) might have had enhanced aerobic capacities because they appear to have been fully terrestrial and cursorial with habitually upright limb posture (17).

References and Notes

1. R. E. Reid, in *The Complete Dinosaur*, J. O. Farlow and M. K. Brett-Surman, Eds. (Indiana Univ. Press, Bloomington, 1997), pp. 449–473.
2. J. A. Ruben, T. D. Jones, N. R. Geist, W. J. Hillenius, *Science* **278**, 1267 (1997).
3. R. Hengst, *ibid.* **281**, 47 (1998).
4. C. Dal Sasso and M. Signore, *Nature* **392**, 383 (1998).
5. _____, in *Third European Workshop of Vertebrate Paleontology-Maastricht*, J. W. M. Jagt, P. H. Lambers, E. W. A. Mulder, A. S. Schulp, Eds. (Naturhistorisches Museum, Maastricht, The Netherlands 1998), p. 23.
6. R. B. Chiasson, personal communication. Figure 2A was drawn from original dissections of three specimens of *Alligator*.
7. H.-R. Duncker, in *Form and Function in Birds*, A. S. King and J. McLelland, Eds. (Academic Press, New York, 1989), vol. 1, pp. 39–67.
8. _____, *Adv. Anat. Embryol. Cell Biol.* **45**, 1 (1971); P. Scheid and J. Piiper, in (7), vol. 4, pp. 369–388.
9. J. McLelland, in (7), vol. 4, pp. 69–100.
10. Under UV illumination [provided with an 80-watt, mercury vapor incandescent bulb (350 to 400 nm)], the dark blue-indigo fluorescence of the liver in *Scipionyx* is distinct from that of any other structure in the specimen or the surrounding matrix. Available

evidence indicates that biliverdin is a predominant liver bile pigment present in nonmammalian tetrapods [T. K. With, *Bile Pigments* (Academic Press, New York, 1968)]. Fluorescence of biliverdin includes a primary light emission peak at about 470 nm, which corresponds to the blue region of the spectrum of visible light [P.-S. Song et al., *J. Am. Chem. Soc.* **95**, 7892 (1973)]. Thus, coloration of *Scipionyx's* liver under ultraviolet illumination is possibly consistent with the presence of liver bile pigment residues in this region of the specimen (P. E. Hare, personal communication).

11. A. S. Romer, *Osteology of the Reptiles* (Univ. of Chicago Press, Chicago, IL, 1956).
12. Under ultraviolet illumination, the texture and fluorescence of these diaphragmatic muscle fibers, although apparently not well fossilized, are distinct from the surrounding matrix and are generally similar to that of previously described portions of the caudofemoralis and pectoral girdle muscles in *Scipionyx*. Identification of this element as a remnant of the diaphragm musculature is based primarily on its lon-

gitudinal, fanlike, fibrous structure and its location in the specimen. Both of these features conform closely to corresponding portions of the diaphragmatic muscle in living crocodylians.

13. D. R. Carrier, personal communication; *J. Exp. Biol.* **152**, 453 (1990).
14. J. A. Ruben et al., *Science* **273**, 1204 (1996).
15. J. W. Hicks and C. G. Farmer, *ibid.* **281**, 45 (1998); J. A. Ruben et al., *ibid.*, p. 47.
16. A. F. Bennett, R. S. Seymour, G. J. W. Webb, *J. Exp. Biol.* **118**, 161 (1985).
17. D. R. Carrier, *Paleobiology* **13**, 326 (1987); E. H. Colbert and C. C. Mook, *Bull. Am. Mus. Nat. Hist.* **97**, 143 (1951).
18. We thank G. Tocco and C. Sloan for assistance in obtaining access to specimens used in this study. Supported by The College of Charleston, Charleston, SC, and an NSF grant IBN-9420290 to W.J.H. and J.A.R.

4 September 1998; accepted 10 December 1998

An ~15,000-Year Record of El Niño–Driven Alluviation in Southwestern Ecuador

Donald T. Rodbell,* Geoffrey O. Seltzer, David M. Anderson, Mark B. Abbott, David B. Enfield, Jeremy H. Newman

Debris flows have deposited inorganic laminae in an alpine lake that is 75 kilometers east of the Pacific Ocean, in Ecuador. These storm-induced events were dated by radiocarbon, and the age of laminae that are less than 200 years old matches the historic record of El Niño events. From about 15,000 to about 7000 calendar years before the present, the periodicity of clastic deposition is greater than or equal to 15 years; thereafter, there is a progressive increase in frequency to periodicities of 2 to 8.5 years. This is the modern El Niño periodicity, which was established about 5000 calendar years before the present. This may reflect the onset of a steeper zonal sea surface temperature gradient, which was driven by enhanced trade winds.

The dramatic effects of the 1997–98 El Niño event have highlighted several shortcomings in our understanding of the El Niño–Southern Oscillation (ENSO) phenomenon (1). These shortcomings include the age of onset of modern ENSO variability, long-term (>10³ years) changes in the frequency of past extreme El Niños and their relation with varying oceanic and atmospheric states, and the frequency and magnitude of the ENSO in Earth's greenhouse future. High-resolution records of prehistoric El Niños are needed to address these questions.

D. T. Rodbell and J. H. Newman, Department of Geology, Union College, Schenectady, NY 12308–2311, USA. G. O. Seltzer, Department of Earth Sciences, Syracuse University, Syracuse, NY 13244–1070, USA. D. M. Anderson, National Oceanic and Atmospheric Administration, Boulder, CO 80303, USA. M. B. Abbott, Department of Geosciences, University of Massachusetts, Amherst, MA 01003–5820, USA. D. B. Enfield, Atlantic Oceanographic and Meteorological Laboratory, National Oceanic and Atmospheric Administration, Miami, FL 33149, USA.

*To whom correspondence should be addressed. E-mail: rodbell@union.edu

Proxy records of prehistoric El Niños have been obtained from a variety of archives, including corals, ice cores, tree rings, flood deposits, beach ridges, archeological middens, and soils (2, 3). However, high-resolution coral and ice core records (4) have been limited to the past two millennia, and longer proxy records of El Niños from the tropical Pacific region are inherently discontinuous (3, 5). Here, we present a high-resolution record of storm-derived clastic sedimentation that spans the past 15,000 years and appears to record El Niño events.

Sea surface temperatures (SSTs) near Guayaquil, Ecuador, are some of the first to warm in the region of upwelling along the coasts of Perú and Ecuador during the onset of an El Niño event (1), and typically, rainfall in this region greatly increases over background levels during the onset of strong to very strong (hereafter, severe) (6) El Niños. The mature phase of El Niño, in which the zonal SST gradient is at a minimum, occurs just as the normal austral summer rainy season in western Ecuador begins. During stron-

REPORTS

ger El Niños, the Walker Circulation is altered so that rising motions occur in parts of the eastern Pacific troposphere that are normally characterized by subsidence and inversion. Under these circumstances, the coastal regions of Ecuador and Perú experience intraseasonal bursts of deep convection and torrential rainfall. For example, during the 1982–83 El Niño, the thermocline began to deepen off the south coast of Ecuador in October 1982, and ocean temperatures abruptly increased 6.2°C at the surface and 9°C at a depth of 50 m (7). Convection-driven precipitation was substantially in-

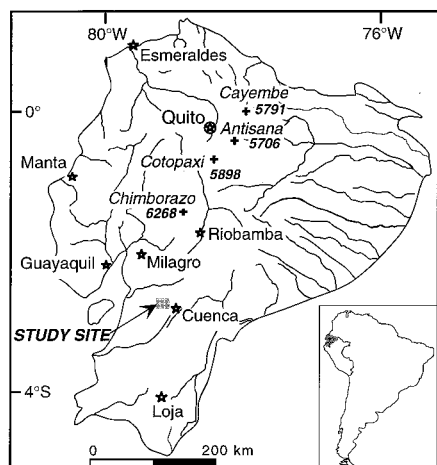


Fig. 1. Location of Laguna Pallacocha is 500 m east of the continental divide in southwestern Ecuador.

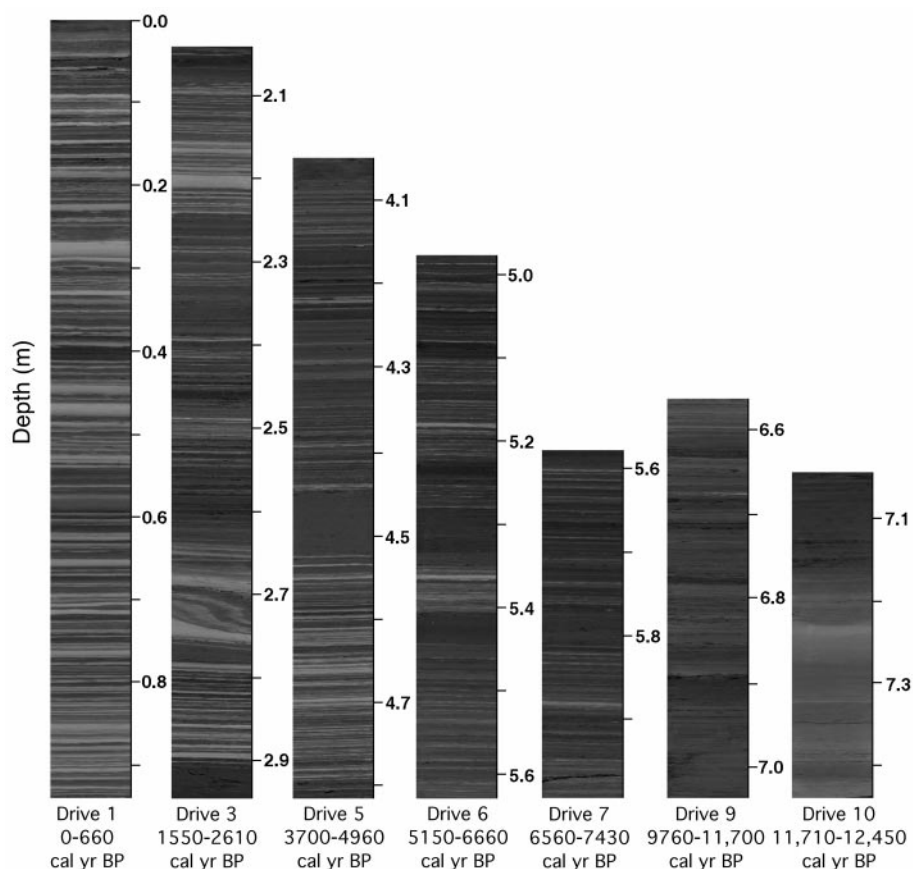
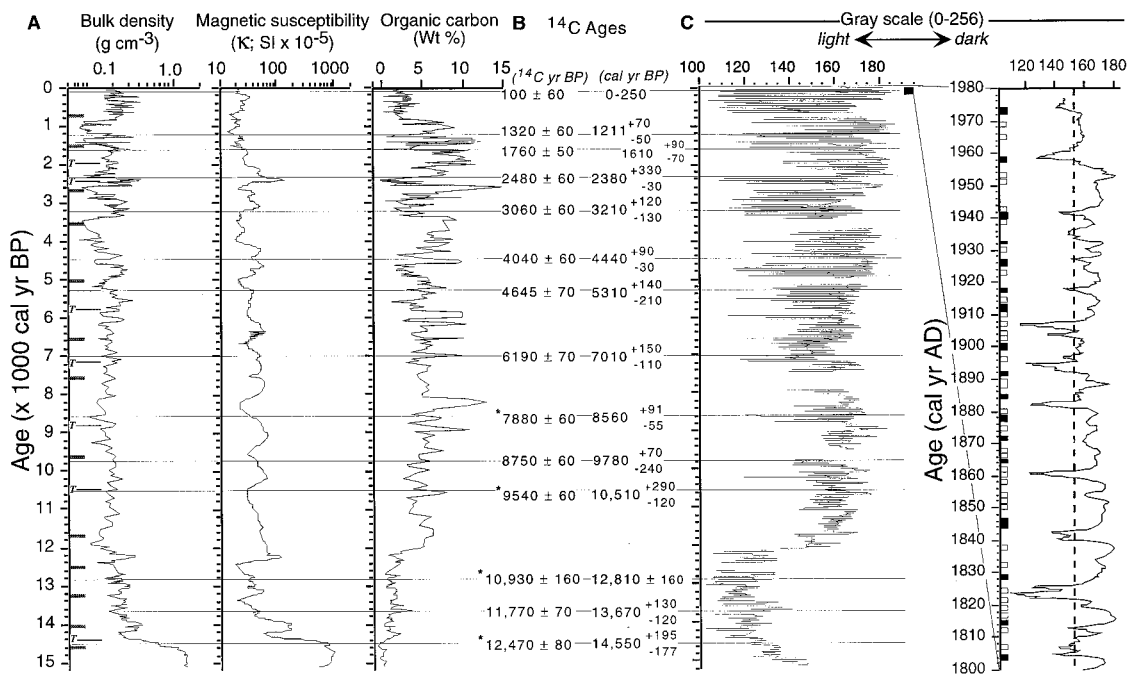


Fig. 2. Photographs of selected sections of the Pallacocha core. Depth scale is meters below the top of the recovered core. The transition from light-colored inorganic sediment, which comprises the Late Glacial interval, to dark organic-rich gyttja occurs ~12,300 cal yr B.P. in the base of drive 10. A progressive increase in the frequency of clastic laminae that are light colored and inorganic occurs throughout the Holocene (for example, drives 10 to 1).

Fig. 3. Downcore variation in (A) bulk density, magnetic susceptibility, and organic C content; (B) ¹⁴C ages; and (C) gray scale. The 14 AMS ¹⁴C ages are from terrestrial plant macrofossils and have been converted to the calendar year time scale with the calibration program of Stuiver and Reimer (27). The ages with an asterisk are from a nearby lake and are correlated to this core by their stratigraphic position in relation to geochemically distinct tephra, which are denoted as T in the left-hand depth scale. Short, stippled horizontal lines in the depth scale denote core section boundaries. The gray scale ranges from 0 (white) to 256 (black) and is primarily controlled by the organic C content of the sediment (14). The age (14) of clastic laminae that are light-colored, inorganic, and <200 years old agrees with the timing of instrumentally or historically documented



occurrences (or both) of severe or moderate El Niños (or both) (solid and open boxes, respectively, in the right-hand depth scale) (6), thus establishing ENSO as a major control on sedimentation in Laguna Pallacocha.

Fig. 4 (below). Age-depth plot for Laguna Pallcacocha. Ages are based on AMS ^{14}C dating of terrestrial macrofossils; symbol size includes a $\pm 1\sigma$ uncertainty in the calendar year calibration (27). The sediment-water interface is assumed to be modern (1993 A.D.). The four solid dots that are plotted along the curve are the ^{14}C ages (denoted with an asterisk in Fig. 3B) that are correlated to this core from a nearby lake on the basis of their stratigraphic position in relation to geochemically distinct tephra (Fig. 3A). Because of a ± 10 -cm uncertainty in the position that these ^{14}C ages correspond with in the Pallcacocha core, we use them only as supporting ages for the chronology of the core, which is based on 9 of the 10 ^{14}C ages that were obtained from Laguna Pallcacocha; because of nonunique calendar year solutions to the youngest ^{14}C date (100 ± 60 ^{14}C yr B.P.) (Fig. 3B), we do not use this date in the age model (14). The progressive increase in sedimentation rates through the early Holocene is due to the increase in input of storm-induced clastic sediment, which reflects the progressive increase in frequency of El Niños through the middle and late Holocene.

creased between 2.5° and 6°S at sites that are as far as several hundred kilometers inland and was increased at elevations from sea level to >3000 m above sea level (masl) (8, 9). Beginning in January 1983, repetitive bursts of extreme rainfall were responsible for much of the devastating flooding that occurred in the region (9). During normal and La Niña years, the Walker Circulation returns to normal, and conditions required for deep convection seldom exist (10).

We analyzed a 9.2-m-long core (obtained in June 1993) that spans the past $\sim 15,000$ calendar years from Laguna Pallcacocha (4060 masl and $2^\circ 46'\text{S}$, $79^\circ 14'\text{W}$) (Fig. 1). The Holocene section contains hundreds of light-colored inorganic, clastic laminae (<0.1 to 1.0 cm thick) that are interbedded with massive organic-rich laminae (Fig. 2). This stratigraphy is reflected in variable bulk density, magnetic susceptibility, C content, and color (11) (Fig. 3, A through C). Sediment records from most similar deglacial lakes in

the tropical Andes reveal an abrupt rise in organic C, which correlates with deglaciation, and a sedimentologically uneventful Holocene interval (12). The 0.05-km^2 lake is located ~ 500 m east of the continental divide in a cirque basin that has been ice free for the past $\sim 14,000$ calendar years. The volcanic bedrock of the region erodes easily, and debris flows and talus are abundant along the divide and are located within several hundred meters of the lake.

The inorganic laminae likely represent deposition from density-driven undercurrents that carried terrestrially derived clastic sediment and some organic matter (13) into the 15-m-deep basin in response to brief storm events that mobilized the abundant loose sediment in the headwaters of the drainage basin as debris flows. The inorganic laminae have $<2\%$ organic C, whereas the organic-rich laminae have $>10\%$ organic C; the inorganic laminae tend to have a coarser modal grain size and contain less biogenic silica than

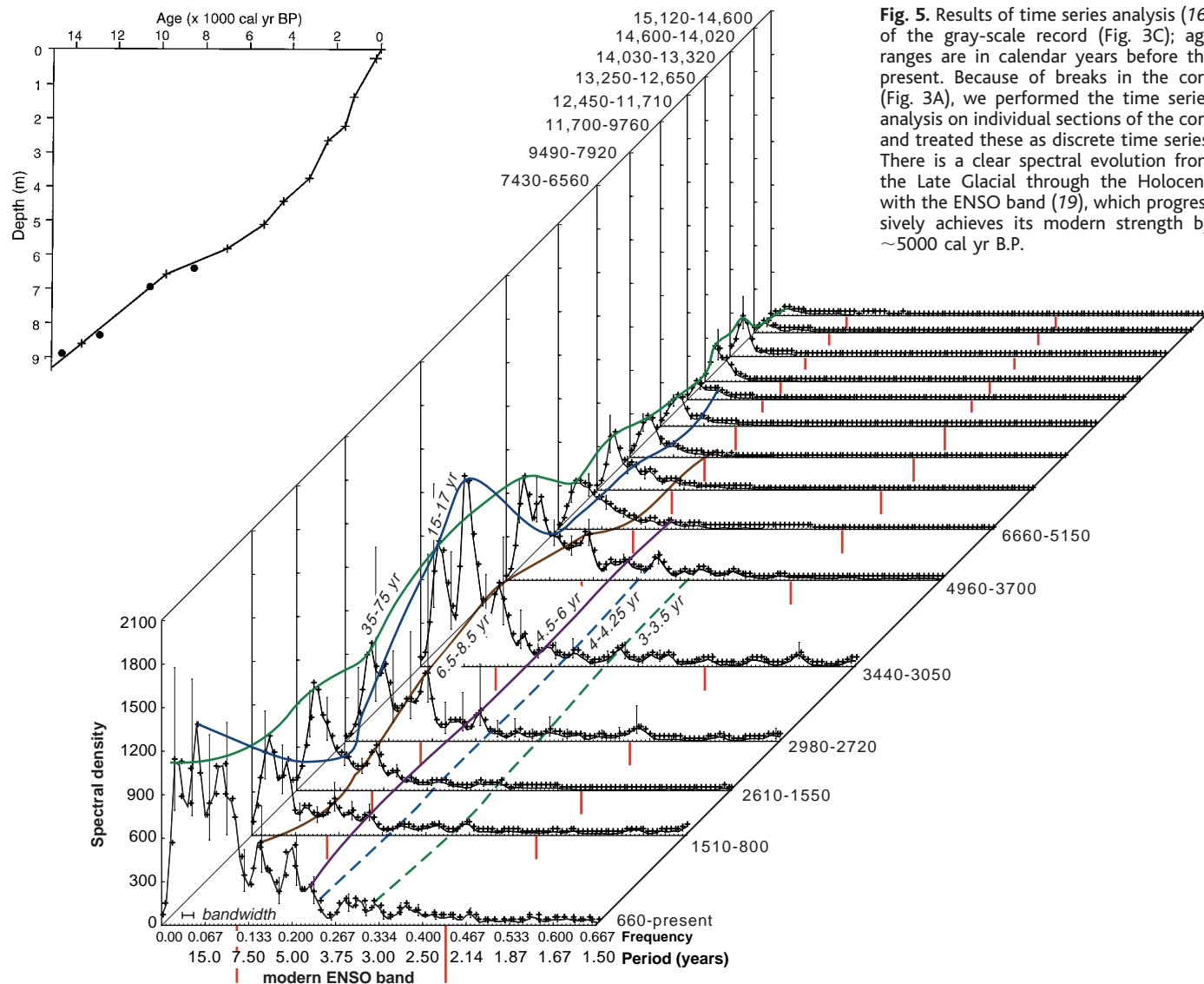


Fig. 5. Results of time series analysis (16) of the gray-scale record (Fig. 3C); age ranges are in calendar years before the present. Because of breaks in the core (Fig. 3A), we performed the time series analysis on individual sections of the core and treated these as discrete time series. There is a clear spectral evolution from the Late Glacial through the Holocene with the ENSO band (19), which progressively achieves its modern strength by ~ 5000 cal yr B.P.

organic-rich laminae (1 to 3% versus 5 to 10%, respectively). Most of the inorganic layers have abrupt basal contacts and fine upward.

The core was dated on the basis of 14 accelerator mass spectrometer (AMS) ¹⁴C ages of terrestrial macrofossils and the identification of seven tephra layers (Fig. 3B). We developed an age model (14) by assuming that the sediment-water interface is modern (1993 A.D.) (Fig. 4) and that, between AMS ¹⁴C-dated intervals (Fig. 3B), the rate of background C deposition was nearly constant and was interrupted by abrupt clastic depositional events, which diluted the C concentration of the sediment. Linear interpolation between dated intervals would result in a substantial underestimation of the time separating the rapidly deposited clastic events. Our constant C flux model (14) essentially removes the clastic laminae from the record, assigns time to the core, and then reinserts the clastic laminae in their correct temporal position.

Analysis of the gray-scale record of the past 660 calendar years (Fig. 2) confirms that the clastic layers reflect El Niño events (15) and depositional events with longer periodicities. The Blackman-Tukey spectrum of the gray-scale record (16) (Fig. 5) reveals concentrations of variance at 1/50 to 1/11, at 1/6.8, and at 1/5 cycles/year; singular spectrum analysis identifies oscillatory pairs with frequencies of 1/25 and 1/10 cycles/year; multitaper and maximum entropy methods (17) also indicate ENSO and decadal band variance. We used the multitaper method (17, 18) to test the null hypothesis that the peaks are red noise; for the ENSO band, we rejected the hypothesis at the 99% level, but we did not reject the red noise hypothesis for the decadal frequency variance.

The sediment record from 1800 to 1976 A.D. reveals a close match (Fig. 3C) between the timing of clastic laminae (low gray-scale value) and moderate to severe El Niño events (6). We estimated that the age uncertainty for this part of the record is $\geq 5\%$ of the age of laminae. Of the 17 severe El Niños that occurred in this time period, 11 correlate within 2 years of major clastic laminae, and 1 is within 3 years of a lamina; we define major clastic laminae as having gray-scale values that are below the mean for the period from 1800 to 1976. The other five severe El Niños of this interval occurred within 2 years of relatively minor clastic laminae. The interval from 1976 to 1993 was disturbed during coring, and thus, we do not have a signal of the 1982–83 event. The eight severe El Niños of the past 100 years (6) correlate precisely with clastic laminae in the core (Fig. 3C). Twenty-six of the 33 moderate El Niños that occurred from 1800 to 1976 A.D. (6) correlate precisely with at least minor clastic layers, as indicated by low or falling gray scale. The mod-

erate El Niños of 1806–07, 1821–24, 1860, 1897, 1904–05, and 1907 correlate with major clastic laminae. Five of these six moderate events follow relatively minor sedimentologic responses to severe events, and thus, it is possible that these moderate El Niños had an anomalously large impact on sediment delivery to Laguna Pallcacocha because of an unusual abundance of fine-grained material left in debris flow channels or along the margin of the lake basin during the preceding severe events.

The full sediment record shows that the frequency of clastic depositional events, which is apparent in the visible stratigraphy (Fig. 2) and time series analysis (Fig. 5), has increased progressively. The periodicity of clastic sedimentation has evolved from ≥ 15 years during the Late Glacial and early Holocene [$\sim 15,000$ to 7000 calendar years before the present (cal yr B.P.)] (Fig. 5). Beginning at ~ 7000 cal yr B.P., clastic events were spaced 10 to 20 and 2 to 8.5 years apart; the 2- to 8.5-year periodicity is most apparent after ~ 5000 cal yr B.P. and is consistent with the periodicity of modern El Niños (19). This increase in clastic input is reflected in average bulk sedimentation rates (Fig. 4). During the Late Glacial ($\sim 10,000$ to 15,000 cal yr B.P.), sedimentation rates averaged 5.2 cm/(100 years). From $\sim 10,000$ to 7000 cal yr B.P., average bulk sedimentation rates dropped to their lowest values of the past 15,000 years [2.7 cm/(100 years)] because the input of glacially derived sediment had ceased and storm-derived sediment input was low. By ~ 7000 cal yr B.P., sedimentation rates began to progressively increase and reached 5.5 cm/(100 years) from ~ 2400 to 1200 cal yr B.P.

The lack of variance in the ENSO band from $\sim 15,000$ to 7000 cal yr B.P. implies that the ENSO was weak, perhaps because the zonal SST gradient was subdued. Because the tropical Pacific behaves as a coupled ocean-atmosphere system (1), a reduction in trade wind circulation is simultaneously the cause of and the consequence of a reduced zonal SST gradient. A weakened zonal SST gradient may have been caused by a smaller and less intense western Pacific warm pool, by warmer SSTs in the equatorial and coastal upwelling zones of the eastern Pacific, or by both.

Recent Sr/Ca ratios and $\delta^{18}\text{O}$ records from the Great Barrier Reef, Australia, indicate that, during the early Holocene, the western Pacific SST was $\sim 1.2^\circ\text{C}$ higher than the present SST (20). Thus, if the apparent reduction in ENSO during the early Holocene was caused by a reduced zonal SST gradient, the reduced gradient must have been caused by elevated SSTs in the eastern Pacific Ocean. Holocene molluscan assemblages in natural deposits and shell middens that were ¹⁴C-dated at >5000 years B.P. (~ 5700 cal yr

B.P.) along the Peruvian coast north of 10°S and along the southern coast of Ecuador are anomalous in that they are dominated by tropical species rather than the temperate species that have inhabited these coastal waters during non-El Niño years for the past 5000 ¹⁴C years (5). The occurrence of these thermally anomalous molluscan assemblages (TAMAs) has been used to infer that the zonal Walker Circulation that is characteristic of normal or La Niña years was reduced during the early Holocene and that the oscillation between El Niño and La Niña states was muted (5, 21). This result is consistent with pollen records from Australasia, which record a middle Holocene onset of the highly variable climate that is produced by ENSO in that region today (22). A warmer eastern Pacific during the early Holocene is also consistent with the $\delta^{18}\text{O}$ record of tropical precipitation obtained from an ice core at Nevado Huascarán in the western cordillera of the Peruvian Andes (9°S and 6048 masl) (23).

Recent modeling results of the coupled ocean-atmosphere system over the tropical Pacific corroborate the occurrence of two oceanic modes in the tropical Pacific (24): one is warm and steady, and the other is cold and oscillating. The model results indicate that development of the cold oscillating mode is dependent on the achievement of a strong temperature gradient between surface water and the main thermocline of the tropical east-central Pacific. Because the temperature of the main thermocline in the east-central Pacific is driven by higher latitude SSTs (25), we hypothesize that the temperature gradient may have increased since 10,000 cal yr B.P. as a consequence of the steadily increasing contrast in seasonal insolation between the equator and high latitudes (26). This model (24) implies that if high-latitude SSTs warm more than tropical SSTs in an enhanced-greenhouse future, ENSO would be reduced with the development of a warm and steady tropical Pacific. Insofar as the early Holocene can be used as an analog for Earth's greenhouse future, our results and those of others (5, 22) lend credence to this scenario.

References and Notes

1. M. J. McPhaden and J. Picaut, *Science* **250**, 1385 (1990); M. A. Cane and S. E. Zebiak, *ibid.* **228**, 1085 (1985); N. E. Graham and W. B. White, *ibid.* **240**, 1293 (1988); E. M. Rasmusson and T. H. Carpenter, *Mon. Weather Rev.* **110**, 354 (1982); D. B. Enfield, *Rev. Geophys.* **27**, 159 (1989).
2. T. J. De Vries, *J. Geophys. Res.* **92**, 14471 (1987); H. F. Diaz and V. Markgraf, Eds., *El Niño: Historical and Paleoclimatic Aspects of the Southern Oscillation* (Cambridge Univ. Press, Cambridge, 1992); L. Martin, M. Fournier, P. Mourguiart, A. Sifeddine, B. Turcq, *Quat. Res.* **39**, 338 (1993).
3. L. E. Wells, *Geology* **18**, 1134 (1990); J. S. Noller, thesis, University of Colorado, Boulder (1993).
4. J. E. Cole, R. G. Fairbanks, G. T. Shen, *Science* **260**, 1790 (1993); R. B. Dunbar, G. M. Wellington, M. W. Colgan, P. W. Glynn, *Paleoceanography* **9**, 291 (1994); L. G. Thompson, E. Mosley-Thompson, B. Mo-

rales Arnao, *Science* **226**, 50 (1984); L. G. Thompson, in *Climate Since A.D. 1500*, R. S. Bradley and P. D. Jones, Eds. (Routledge, London, 1992), p. 517–548.

5. D. H. Sandweiss, J. B. Richardson III, E. J. Reitz, H. B. Rollins, K. A. Maasch, *Science* **273**, 1531 (1996); *ibid.* **276**, 966 (1997).
6. W. H. Quinn and V. T. Neall, in *Climate Since A.D. 1500*, R. S. Bradley and P. D. Jones, Eds. (Routledge, London, 1992), pp. 623–648.
7. E. Cicaloni, *J. Geophys. Res.* **92**, 14309 (1987).
8. J. D. Horel and A. G. Cornejo-Garrido, *Mon. Weather Rev.* **114**, 2091 (1986).
9. R. A. Goldberg and G. Tisnado, *J. Geophys. Res.* **92**, 14225 (1987).
10. G. S. Philander, *J. Atmos. Sci.* **42**, 2652 (1985).
11. We photographed cores digitally and processed these images with the National Institutes of Health program IMAGE. This program assigns a value between 0 (white) and 256 (black) to each pixel. Because each pixel represents ~0.3 mm of core and because gray scale is a good proxy for C content, the gray-scale record represents a proxy for the oscillation between inorganic, storm-induced clastic sedimentation and organic-rich background sedimentation with subannual resolution.
12. D. T. Rodbell, *Geol. Soc. Am. Bull.* **105**, 923 (1993).
13. The geochemistry of the organic matter indicates that most of the C supplied to the lake was derived from terrestrial sources during the deposition of light and dark laminae, as there is little difference between the organic matter contained in the two types of laminae. All the free and bound aliphatic biomarkers in both the light and dark laminae are dominated by *n*-alkanes ranging in C chain length from C₂₁ to C₃₅. The chain length and a pronounced odd-over-even dominance suggest a terrestrial plant source, and the suite of biomarkers present is almost exclusively from a terrestrial plant source. These results are corroborated by similar C/N ratios and δ¹³C values for both light and dark laminae.
14. Gray scale is a proxy indicator of C content ($Y = 10^{-14}X^{6.628}$, where *Y* is weight % of C and *X* is gray scale; *n* = 32 samples), and C content is a proxy for sediment bulk density ($Y = 0.282X^{-0.338}$, where *Y* is bulk density and *X* is weight % of C; *n* = 447 samples). Correlation coefficients for these equations are 0.89 and 0.82, respectively, and both exceed critical values at the 99.9% confidence level. From these equations, the mass of C represented by each pixel in the digital record can be estimated, and the total mass of accumulated C between dated intervals can be determined. From the total mass of C, the average rate of C deposition can be calculated, and time can then be allocated between AMS ¹⁴C-dated intervals according to the gray-scale value, so that the lighter the color of sediment, the less time it represents (and vice versa).
15. The El Niño signal that is recorded in Laguna Pallcacocha may be complicated by other factors. Delta progradation may influence the delivery of clastic sediment to the deep basin, and we expect that this would cause a progressive increase in the grain size and thickness of the clastic layers; however, we have noted no such trends. Seismic activity may be responsible for clastic events, but it is unlikely that this would have a major effect on the periodicity of sedimentation within the 2- to 8.5-year ENSO band. Because most precipitation that falls in the tropical Andes is derived from the tropical easterlies, it is possible that the North Atlantic Oscillation is a compounding influence on interannual sediment delivery to the lake [Y. Kushnir, *J. Clim.* **7**, 141 (1994)].
16. The time series for each drive were interpolated at a 0.75-year interval (the minimum sample spacing). The trend and low-frequency variance were removed with a triangular-shaped filter with a 1/2 pass band frequency of 1/150 year. With 100 lags ($M = n/8$, where *M* is the number of lags), we calculated the variance spectrum as the Fourier transform of the autocovariance function, using the Blackman-Tukey method [G. M. Jenkins and D. G. Watts, *Spectral Analysis and Its Applications* (Holden-Day, Oakland, CA, 1968)] in the ARAND package from Brown Uni-

versity (Providence, RI). Confidence levels (80%) are based on the inverse chi-square distribution.

17. R. Vautard, P. Yiou, M. Ghil, *Physica D* **58**, 95 (1992).
18. D. J. Thompson, *Philos. Trans. R. Soc. London Ser. A* **330**, 601 (1990).
19. D. B. Enfield and L. Cid, *J. Clim.* **4**, 1137 (1991); K. E. Trenberth, *Bull. Am. Meteorol. Soc.* **78**, 2771 (1997); M. J. McPhaden et al., *J. Geophys. Res.* **103**, 14169 (1998).
20. M. K. Gagan et al., *Science* **279**, 1014 (1998).
21. On the basis of flood deposits intercalated with clay-enriched aridic soils along the hyperarid north coast of Perú, an alternative interpretation has been proposed, which asserts that the presence of TAMAs is a result of coastal geomorphology and sea-level rise rather than climate [T. J. DeVries, L. Ortlieb, A. Diaz, L. Wells, Cl. Hillaire-Marcel, *Science* **276**, 965 (1997); L. E. Wells and J. S. Noller, *ibid.*, p. 966] and that the ENSO persisted through at least the past 40,000 years (3). Our record clearly shows that storm-generated clastic depositional events occurred during the Late Glacial and early Holocene with periodicities of ≥15 years, but not in the 2- to 8.5-year ENSO band. The interpretation of the TAMA (5) is also problematic because it implies a quasi-permanent El Niño state, which is neither evident in our record as a prolonged period of clastic sedimentation, nor in other proxy records from the region (3). We suggest that whereas El Niños may have been less frequent, the eastern

Pacific was marked by less intense upwelling and zonal circulation and was capable of producing infrequent and localized coastal flooding but was insufficient to generate high-frequency convective-driven precipitation to 4000 masl.

22. M. S. McGlone, A. P. Kershaw, V. Markgraf, in *El Niño: Historical and Paleoclimatic Aspects of the Southern Oscillation*, H. F. Diaz and V. Markgraf, Eds. (Cambridge Univ. Press, Cambridge, 1992), pp. 434–462; J. Shulmeister and B. G. Lees, *Holocene* **5**, 10 (1995).
23. L. G. Thompson et al., *Science* **269**, 46 (1995).
24. D.-Z. Sun, in *El Niño and the Southern Oscillation: Multiscale Variability, Global and Regional Impacts*, H. F. Diaz and V. Markgraf, Eds. (Cambridge Univ. Press, Cambridge, in press).
25. G. L. Pickard and W. J. Emery, *Descriptive Physical Oceanography* (Pergamon, Oxford, 1982).
26. A. Berger, *Quat. Res.* **9**, 139 (1978).
27. M. Stuiver and P. J. Reimer, *Radiocarbon* **35**, 215 (1993).
28. We thank R. Fleischer, P. Gremillion, and anonymous reviewers for improving the manuscript and C. Oballe and K. Reed for their help in retrieving the sediment core. Supported by NSF grants EAR9418886 (D.T.R.) and EAR9422424 (G.O.S.) and by the Union College Internal Education Foundation (J.H.N.) and Faculty Research Fund (D.T.R.).

20 October 1998; accepted 11 December 1998

Nanophase-Separated Polymer Films as High-Performance Antireflection Coatings

Stefan Walheim, Erik Schäffer, Jürgen Mlynek, Ullrich Steiner*

Optical surfaces coated with a thin layer to improve light transmission are ubiquitous in everyday optical applications as well as in industrial and scientific instruments. Discovered first in 1817 by Fraunhofer, the coating of lenses became standard practice in the 1930s. In spite of intensive research, broadband antireflection coatings are still limited by the lack of materials with low refractive indices. A method based on the phase separation of a macromolecular liquid to generate nanoporous polymer films is demonstrated that creates surfaces with high optical transmission.

Light reflection off glass surfaces is undesirable, disturbing, and limits the performance of devices for which maximum light transmission is required (such as solar cells). Anti-reflection (AR) coatings reduce the intensity of reflection and increase the quality of optical lens systems. The basic principle of optical coatings can easily be understood as follows (1). The reflected light from the air-film and film-substrate interfaces must interfere destructively to maximize the light transmission into the transparent substrate (Fig. 1A). Two conditions must be met: (i) The light amplitudes reflected at both interfaces must be equal; that is, $n_0/n_f = n_f/n_s$ or $n_f = \sqrt{n_0 n_s}$, with n_0 , n_f , and n_s being the refractive indices of air, film, and

substrate respectively; and (ii) the optical path length must be chosen for the reflected wave to interfere destructively; that is, the film thickness must be 1/4 of a reference wavelength in the optical medium. Although condition (ii) can be easily met, condition (i) poses a problem: Refractive indices for glass and transparent plastic substrates are ≈1.5, therefore requiring that $n_f \approx 1.22$. Because the lowest refractive indices for dielectrics are on the order of 1.35, single-layer AR coatings cannot attain this value. For broadband AR coatings, a sequence of layers is needed that have refractive indices varying stepwise from n_0 to n_s . In this case, $n_f < 1.22$ is desirable.

Instead of a homogeneous layer, a nanoporous film can be used. If the pore size is much smaller than the visible wavelengths, the effective *n* of the nanoporous medium is given by an average over the film. The challenge is to maximize the volume ratio of pores in order to achieve the refractive indi-

Fakultät für Physik, Universität Konstanz, D-78457 Konstanz, Germany. www.uni-konstanz.de/FuF/Physik/Mlynek/Steiner/

*To whom correspondence should be addressed. E-mail: ulli.steiner@uni-konstanz.de